Electrical Behavior of Polyurethane Derived from Polyols Synthesized with Glycerol, Phthalic Anhydride, and Oleic Acid

T. S. Velayutham,[1] W. H. Abd Majid,[1] S. N. Gan[2]

[1]*Low Dimensional Materials Research Centre, Physics Department, University of Malaya, 50603 Kuala Lumpur, Malaysia*
[2]*Chemistry Department, University of Malaya, 50603 Kuala Lumpur, Malaysia*

Received 17 February 2010; accepted 27 September 2010
DOI 10.1002/app.33468
Published online 8 March 2011 in Wiley Online Library (wileyonlinelibrary.com).

ABSTRACT: The direct current (DC) and alternating current (AC) conductivity of polyurethane (PUR) derived from polyols synthesized with glycerol, phthalic anhydride, and oleic acid were investigated in this article. The PUR was prepared by varying the oleic acid content in polyol (28, 40, and 65%) and the NCO/OH ratio of the PUR was varied to 1.2, 1.4, and 1.6. The electrical conduction studied by measuring the dependence of current on the applied field and temperature. Electrical conductivity in PUR was expressed by Arrhenius relations and the activation energies were calculated. Moreover, hyperbolic sine function was used to determine the conduction mechanism in PUR. It's presumed that the conduction mechanism was assisted by ions for the PUR which were contributed by oleic acid due to dissociation of protons and highly polar urethane groups in PUR. Furthermore, the dielectric behaviors of the material have been measured at room temperature in the frequency range of 100 Hz to 40 MHz. The frequency-dependent conductivity of PUR materials has been analyzed using a Jonscher's power law expression and the plot exhibits the typical behavior of ionic materials, i.e., the DC plateau and the frequency dependent region. © 2011 Wiley Periodicals, Inc. J Appl Polym Sci 121: 1796–1803, 2011

Key words: polyurethane; coatings; oleic acid; polyols; electrical properties

INTRODUCTION

Generally, the electrical properties of polymers were studied as a function of frequency, temperature, pressure, plasticizer concentration, and degree of polymerization.[1–3] One of the powerful techniques to investigate the dynamic properties of material is dielectric relaxation spectroscopy. This technique can be applied to polar materials and seems to be ideal for studies of the linear and branched PUR systems.[4–10]

PUR have been intensively studied for many years and have wide applications.[11] Almost all commercial PUR were obtained from petroleum derivatives. Presently, the scientific community has become very interested in developing material that originates from renewable resources. The main vegetable oil used to manufacture PUR of excellent properties is castor oil.[12] There are other oils such as soya,[13] sunflower,[14] linseed,[15] canola,[16,17] and safflower[18] used in the production of PUR. The polyurethane synthesized and investigated in this article is derived from palm oil-based oleic acid polyols which is new in the market. In our previous paper we showed the synthesis and mechanical properties of the oleic acid-based polyol polyurethane with varied oleic acid percentages in polyols and varied NCO/OH ratio of the PUR.[19,20] This article will concentrate on the electrical properties of the material. The effect of oleic acid content in the polyols and NCO/OH ratios of PUR on the electrical properties of the PUR, were investigated in this article.

EXPERIMENTAL DETAILS

Materials

Oleic acid (purity 99.5%) and glycerol (purity 99.5%) were obtained from Cognis Oleochemical (M) Sdn. Bhd (Malaysia). Phthalic anhydride, PA (P.T. Petrowidada, Indonesia) and toluene diisocyanate, TDI (Aldrich, USA) (80 : 20; 2,4-toluene diisocyanate : 2,6-toluene diisocyanate) mixture of the two isomers were used as received. Toluene (JT Baker, USA) was used as solvent; it was dried over activated molecular sieve overnight before use. Silicone surfactant used was L6900 (Air Products, USA) and defoamer BYK-088 was from BYK Chemie, Germany.

Correspondence to: T. S. Velayutham (t_selvi@um.edu.my).
Contract grant sponsor: University of Malaya; contract grant number: Vot F F0161/2004, Post doctoral fellowship, University Malaya.

TABLE I
Activation Energies Derived from Arrhenius Plot

	NCO/OH ratio	Activation energy [E_a (eV)]
PUalk28	1.2	0.80 ± 0.07
	1.4	0.95 ± 0.06
	1.6	0.92 ± 0.05
PUalk40	1.2	1.01 ± 0.08
	1.4	1.0 ± 0.1
	1.6	1.1 ± 0.1
PUalk65	1.2	1.16 ± 0.09
	1.4	1.25 ± 0.04
	1.6	1.7 ± 0.1

Synthesis of polyester polyol and polyurethane

The synthesis of polyols from oleic acid and polyurethane is described in detail in Refs. 19 and 20. The formulations of polyols were based on the method as described in Ref. 21. Preweighed PA, glycerol, and oleic acid were charged into a 2-L four necked round bottom reactor flask and was stirred and heated up to a temperature of 120 to 130°C while a slow stream of nitrogen gas was bubbled through the mixture for 30 min. The temperature was then increased to 180–200°C when the reaction could proceed readily with the evolution of water, which was collected at the decanter arm. The reaction was considered complete after the water of reaction collected was as predicted in the formulation. Three different formulations of polyols were synthesized by varying the content of oleic acid to 28, 40, and 65%. The samples were named as Alk28, Alk40, and Alk65, respectively, in accordance to the percentage of oleic acid in the samples. The compositions and characteristic of the polyols were summarized in Tables I and II in Ref. 19.

Synthesis of PUR were proceeded where the polyol and additives were dried under reduced pressure at 80°C for 2 h before being poured into a three necked flat bottom flask equipped with thermometer, dropping funnel, and magnetic stirrer. The polyol was allowed to react with a calculated amount of TDI in the presence of solvent, toluene, surfactant, and defoamer. TDI was added drop wise into the reaction mixture at 80°C over 3 h with constant stirring. The partially reacted sample formed a viscous solution, which was then poured into a rectangular mold of 12 cm × 12 cm to cure under ambient temperature overnight to form film of 0.5 mm thickness and left in the oven at 60°C for 2 days to evaporate off all the solvent. The NCO/OH ratios of the samples were varied to 1.2, 1.4, and 1.6. For electrical conductivity measurements circular discs with diameter 9 mm and thickness of about 0.5 mm were prepared. While for measurement of dielectric properties, circular disc with diameter 38 mm and thickness of about 0.5 mm were used.

Measurement of electrical properties

The volume electrical conductivity in PUR was measured according to ASTM D257. The samples were measured using a Keithley Source Measurement Unit (Keithley SMU 236, USA) with voltage level varied in the range of 0–100 V. The measurements were performed on the samples placed in the cryostat connected to the temperature controller (Lakeshore 330 Autotuning Temperature Controller, USA) covering a broad temperature range from 28 to 120°C with a resolution of ±0.04°C. The equilibrium time for each temperature was at least 10 min. The samples were sandwiched between the two brass electrodes, one of which was provided with a guard ring. The experiment was performed in vacuum to ensure good electrical contact with the samples.

RESULTS AND DISCUSSION

Electrical conductivity

Electric conductivity in large polymer materials is generally expressed by Arrhenius relations which is

$$\sigma = \sigma_0 e^{(-E_a/kT)} \tag{1}$$

where σ is the value of the electrical conductivity at an absolute temperature T, σ_0 is the conductivity value at absolute zero as obtained by extrapolation, k is the Boltzmann constant and E_a is the activation energy of the conduction process. The activation energy, E_a has a linear correlation with log σ_0 in the form of

$$\log \sigma_0 = A + BE_a \tag{2}$$

which is called the compensation law or Meyer-Neldel rule.

The temperature dependence of electric conductivity in PUR are shown in Figure 1 which manifests the significant influence of the oleic acid content and

TABLE II
The Experimental and Fitted Results of DC Conductivity at Room Temperature Derived from Power Law Plots

	NCO/OH ratio	Experimental σ_{dc} values ($\times 10^{-11}$) ± 0.1 Sm^{-1}	Fitted σ_{dc} values ($\times 10^{-11}$) ± 0.02 Sm^{-1}
PUalk28	1.2	31.6	33.90
	1.4	36.6	35.30
	1.6	37.8	36.80
PUalk40	1.2	3.6	3.31
	1.4	3.3	2.94
	1.6	3.9	3.32
PUalk65	1.4	4.0	3.85
	1.6	7.4	7.15

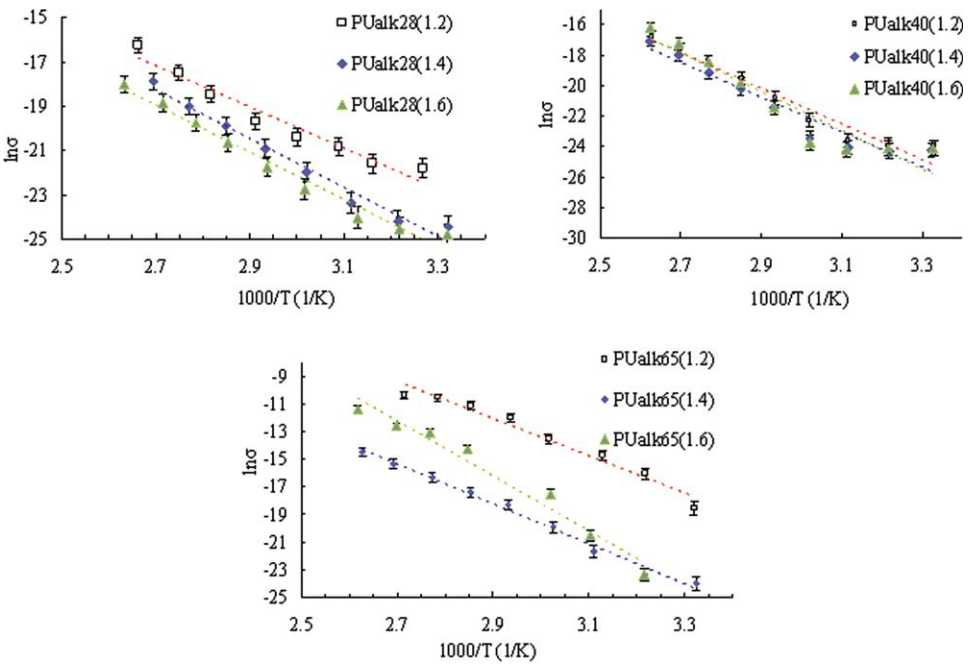

Figure 1 The temperature dependence of electric conductivity in PUR. [Color figure can be viewed in the online issue, which is available at wileyonlinelibrary.com.]

NCO/OH ratios on the electric conductivity. From the slope of the straight lines in Figure 1, activation energies E_a were evaluated and reported in Table I.

The E_a increases as the oleic acid content of the polyols increased. The phase present in larger amount will form continuous matrix and control most of the properties of the sample. For PUalk65, the polyols contain a higher percentage of oleic acid and thus, presumably the higher amount of side chain resulting copolymer separate into micro-phase. The conduction mechanism occurs in PUalk65 is dependent on the oleic acid content and crosslinking due to increase in NCO/OH, thus there is a competing effect between them. The carriers in the micro-phase segments no longer possess the freedom of movement, being trapped or more firmly bound, thus reducing the overall number of carriers. Thus, potential barrier increases causing the E_a to increase.

A decrease in NCO/OH ratio has led to a decrease in the E_a for PUalk65. However, the same trend was not observed for PUalk28 and PUalk40. Presumably there is less crosslinking at lower NCO/OH ratio, hence there is higher free volume and the frequency of the motions, which favors the hopping of the carriers and modifies the height of potential barriers for PUalk65. As for the PUalk28 and Pualk40, the result doesn't follow the trend presumably due to the fact that both of them have much lower oleic acid content.

In PUR it is understood that the charge carrier was pre-existent in the polymer and not being thermally created.[22] Consequently, the temperature only influences the rate of hopping i.e., the carrier mobility. The free carriers which exhibit electrical conductivity in polymers may be ions or electrons. These free carriers may have existed in the polymer medium and they can either hop from site to site or move through a conduction band under the influence of an applied electrical field. If an ionic mechanism is assumed, the greater conductivity at the elevated temperature can be accounted for by the presence of a greater number of ions.[23] The source of this may be ionic dissociation; the number of ions increasing exponentially with temperature. Another possibility is that the mobility of the ions is also enhanced due to a drastic reduction in the internal viscosity of the polymer as the temperature is increased.

To clarify conduction mechanism at the specified field, a wide variety of plots of the current versus voltage relationship have been fitted in the present work; exponential plot,[24] space-charge limited conduction (SCLC) plot,[25] Schottky plot,[26,27] Poole plot,[28] Poole-Frenkel plot,[29] and hyperbolic sine function.[30,31] Of these, the exponential, Schottky, and hyperbolic sine function plots are shown in Figures 2–4. The rest of the plots did not yield satisfactory fitting therefore they were not shown in this article.

Figure 2 shows the typical field dependence of current density, $J(E)$ at various temperatures where $J(E)$ is ohmic at low electric field and nonohmic at high fields. This feature indicates the lowering of lifetime of the trapped carriers in defect or localized states with increasing temperature, which increases

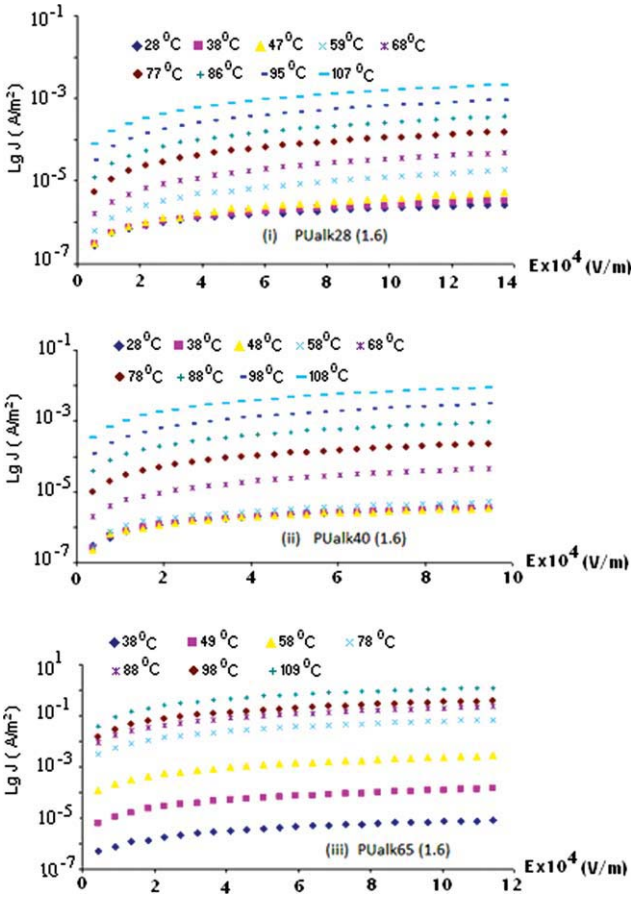

Figure 2 Exponential plot at various temperatures for (i) PUalk28 (1.6), (ii) Pualk40 (1.6), (iii) Pualk65 (1.6). [Color figure can be viewed in the online issue, which is available at wileyonlinelibrary.com.]

the density of free carriers. Consequently, the transition from ohmic to nonohmic behavior occurs at high temperature and field.

Figure 3 shows the plot of current density as function of $E^{1/2}$ (Schottky plot) at various temperatures ranging from 28 to 110°C. The Schottky emission mechanism is an electrode-limited conduction, occurring at low voltages at which the electrons on the surface of the injecting electrode transit above the potential barrier. The experimental results does not show a linear variation of $J(E)$ with respect to $E^{1/2}$ over a wide range of temperature and fields.

The nonlinear behavior of the Schottky plot in Figure 3 at the high fields and temperature can be considered in terms of the hopping mechanism.[32,33] Generally, a free volume of polymer is increased with an increase in temperature. The increase in free volume can facilitate the motion of ionic charges in the bulk. By the high external field, ionic carriers move to the electrode and accumulate on the interface between the bulk and electrode, resulting in a diminishing ionic concentration in the bulk and decrease in the conduction current.[31]

Typical hyperbolic sine function model fit performed on the experimental data were well-matched with hyperbolic sine function eq. (3) as shown in Figure 4. This phenomenon suggests that ion hopping is presumably the predominant conduction mechanism for the PUR.

Ionic conduction by migration of ions by hyperbolic sine function,[30,31]

$$J = (2ne\lambda\delta)\exp\left(-\frac{\phi}{kT}\right)\sinh(\lambda eE/2kT) \qquad (3)$$

where n is the concentration of ion, e is the electronic charge, λ is the hopping distance of ion, δ is the attempt-to-escape frequency, ϕ is the barrier height, E is the electric field, k is the Boltzmann constant, and T is the absolute temperature.

Figure 4 shows the typical hyperbolic sine function model fit performed on PUalk28, PUalk40, and PUalk65 for NCO/OH ratios 1.6 at various temperatures. The experimental values are represented by the dotted points and continuous lines correspond to simulated fit. The experimental data were well-

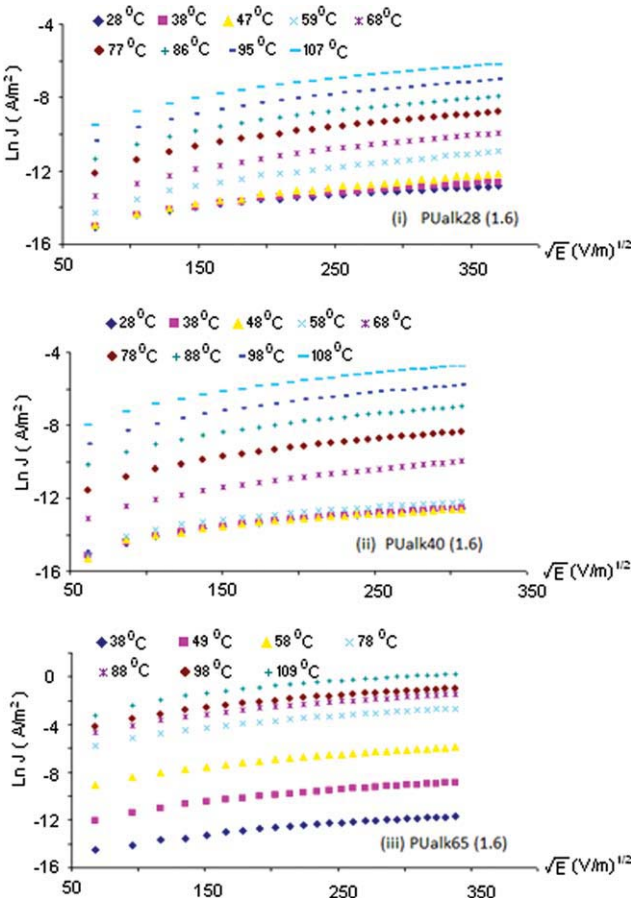

Figure 3 Schottky plot at various temperatures for (i) Pualk28 (1.6), (ii) Pualk40 (1.6), (iii) Pualk65 (1.6). [Color figure can be viewed in the online issue, which is available at wileyonlinelibrary.com.]

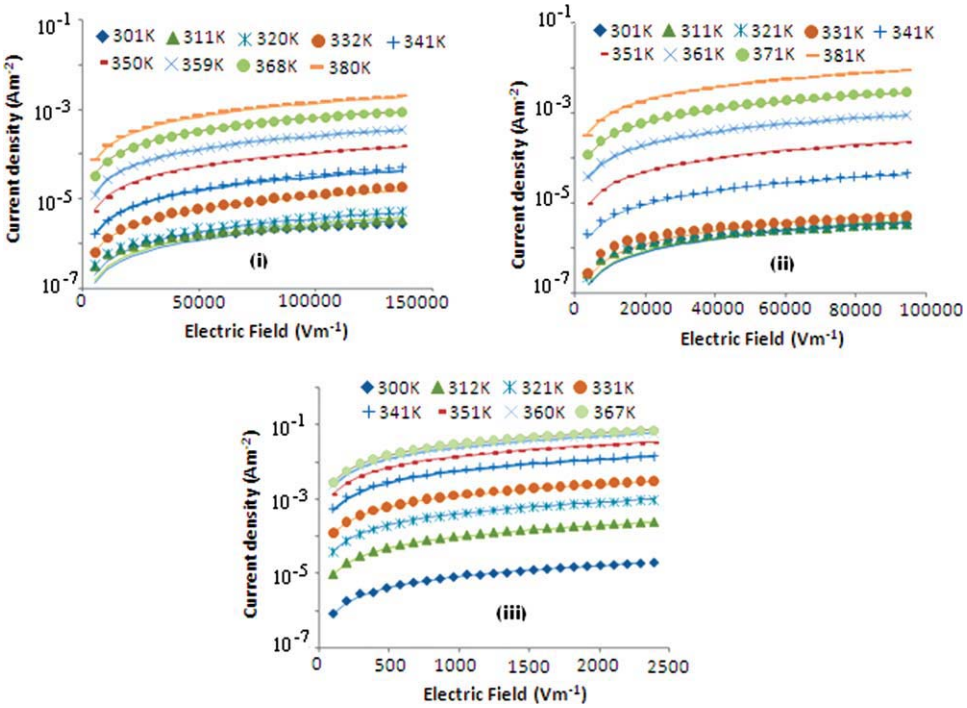

Figure 4 Typical hyperbolic sine function model fit performed on (i) Pualk28 (1.6), (ii) Pualk40 (1.6), and (iii) Pualk65 (1.6). Dots are experimental points and continuous lines corresponds to simulated fit. [Color figure can be viewed in the online issue, which is available at wileyonlinelibrary.com.]

matched particularly at field regions above 500 Vm^{-1} with hyperbolic sine function, eq. (3). This phenomenon suggests that ion hopping is presumably the predominant conduction mechanism above 500 Vm^{-1} field regions for the PUR.

The conduction mechanism in the PUR samples presumably to be ionic due to protons originating from oleic acid content in the samples. In ionic conduction, the current is determined by the migration of ions and expressed by hyperbolic sine function [eq. (3)]. Figure 4 show the results of theoretical (solid line) and experimental data under the ionic conduction at various temperatures. When conduction by an ionic mechanism takes place, the conduction ion moves from one interstitial position to the next as when it acquires sufficient energy to overcome the potential energy barrier. The jump distance from one position to the next was calculated from the hyperbolic sine relationship between the current and voltage of PUR. From these results, the hopping distance is evaluated. Figure 5 shows the plot of hopping distance λ as a function of T ranging from 300 to 380 K. In the present case, $\lambda(T)$ increases gradually as T rises.

Figures 5[A(i)–A(iii)] show the effects of NCO/OH ratios on the hopping distance of PUR. It is noticed that for PUalk28, the hopping distance is almost the same below 360 K for all the NCO/OH ratios. Above 360 K, PUalk28 (1.2) has the highest hopping distance followed by PUalk28 (1.6) and PUalk28 (1.4). As for PUalk40, a similar trend is observed as in PUalk28, where the hopping distance is almost the same for all the samples below 360 K, but above 360 K, the hopping distance is higher for PUalk40 (1.2). However, as the temperature increased further, the hopping distance of PUalk40 (1.6) eventually increased above that of PUalk40 (1.2) and PUalk40 (1.4). As for PUalk65, PUalk65 (1.2) has the highest hopping distance followed by PUalk65 (1.6) and PUalk65 (1.4) along the investigated temperature range.

The variation of λ in temperature has been often observed in the case of other organic polymer.[34] Furthermore, the values estimated by different authors vary considerably and the ionic jump distance may show strong or moderate variation with T depending on the charge carriers. An electron can travel over a large distance particularly in regular lattice but an ion is a relatively massive particle which hops into an adjacent site, unlikely to travel over a large distance. The results obtained in this research support the ionic conduction by migrations of ions since the hopping distance obtained for all the PUR samples were below 10 nm which is considered as a small distance.[34]

The charge carriers or ions were from the system itself. Self ionization of urethane groups[35] and protons originating from oleic acid can be a potential source of ions. The protons from self ionization of urethane groups can contribute to conductions above

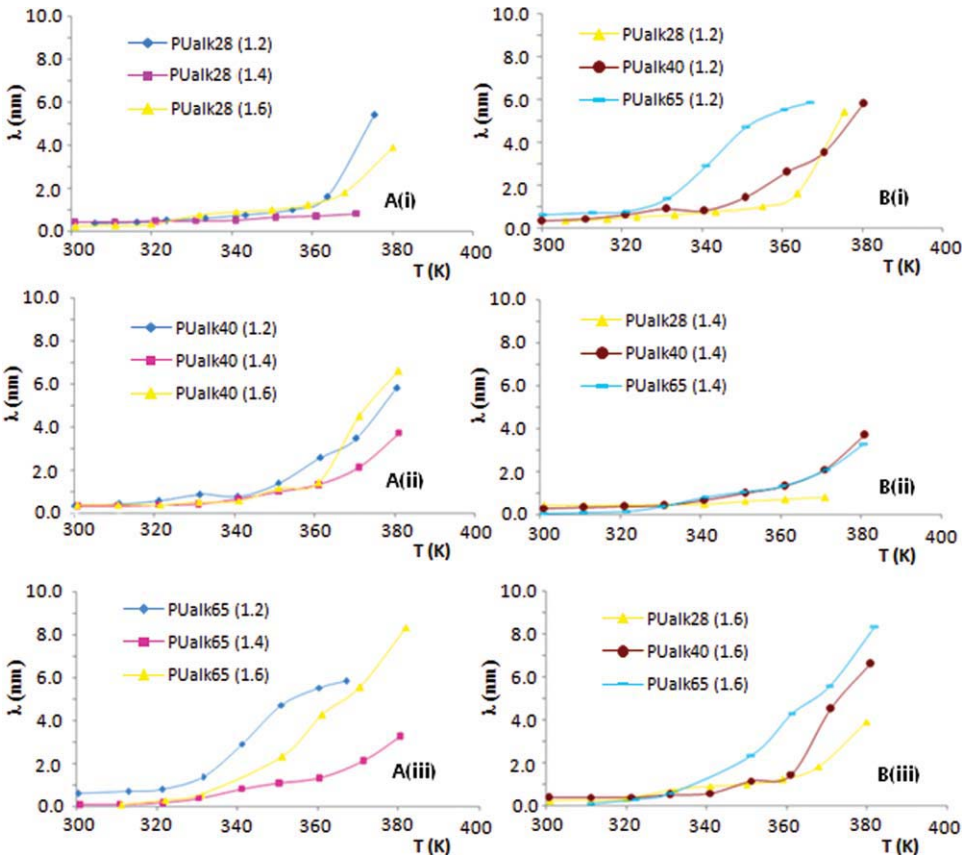

Figure 5 Plot of hopping distance, λ as a function of temperature for varied (A) NCO/OH ratio and (B) oleic acid content. [Color figure can be viewed in the online issue, which is available at wileyonlinelibrary.com.]

glass transition temperature of hard segments where their mobility is greater. When the temperature increases their contribution to conductivity also increases. Protonic contribution increases with temperature due to the gradual removal of constraints on proton mobility.[35] The thermal stability of the polymer film after curing was studied in an N_2 environment using a thermogravimetric analysis (TGA) instrument (Rheometric Scientific, Model 1000+) at a heating rate of 20°C min^{-1} from room temperature to 900°C. Calorimetric measurements were carried out using differential scanning calorimetry (DSC 6, Perkin–Elmer) from 35 to 150°C at 20°C min^{-1}. The T_g for all the PURs were around 123°C and the rapid weight loss of PURs occurred approximately around 170°C which is above the T_g of the samples.

Basically, as NCO/OH ratio increases, the crosslinking increases and thus the localized bonding force between neighboring chains also increases. This could result in small spacing for movement of ions in the bulk with the ion hopping becoming easy. Therefore, it is assumed that the hopping distance is higher for PUR with lower NCO/OH ratio compared to PUR with higher ratios. Moreover, the hopping distance is also affected by the contribution of protons from the oleic acid content in the polyols. As the oleic acid content increases in the samples, the protonic contribution may increase. Consequently, as the temperature increases, the number of protons increases with temperature thus increasing the hopping distance. Another possibility is that the mobility of the ions is increased by the reduction of internal viscosity of the polymer as the temperature increases.

AC conductivity

The frequency dependence of the total ac conductivity is depicted in Figure 6. The conductivity is found to be frequency independent in the low frequency region and DC conductivity, σ(0), has been extracted from the region. Each curves shows the frequency behavior described through Jonscher's universal power feature[36] which is

$$\sigma(\omega) = \sigma(0) + A\omega^n \tag{4}$$

where σ(0) is the DC conductivity of the material, A is the dispersion parameter, and $0 < n < 1$ is the dimensionless frequency exponent. Equation 4 has been used to fit the ac conductivity data where A

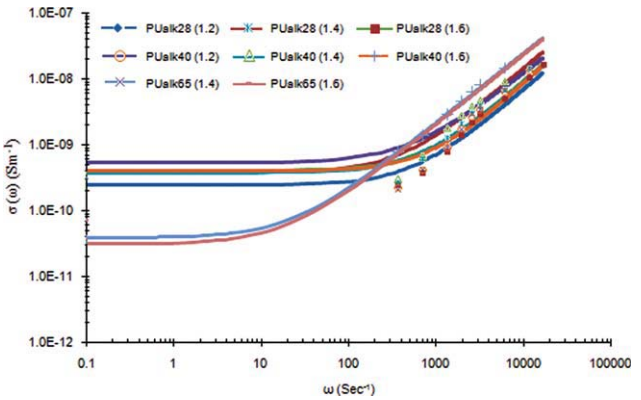

Figure 6 Frequency-dependent conductivity, σ(ac) versus frequency for PUR at room temperature. Dots are experimental points and continuous lines correspond to simulated fit. [Color figure can be viewed in the online issue, which is available at wileyonlinelibrary.com.]

and n values were varied simultaneously to get the best fit.

The fitted curves are shown in the Figure 6. It was found that the fit was satisfactory in all cases. Extrapolation of the fitted results to zero frequency gives DC conductivity, σ_{dc}, which were tabulated in Table II. These results are comparable with commercially available pure PUR which were in the range of 10^{-9} to 10^{-12} Sm^{-1}.[37–40]

Dc conductivity values were measured experimentally by using Keithley Source Measurement Unit (Keithley SMU 236, USA) at room temperature. The validity of the σ_{dc}, values which have been obtained experimentally to the fitted σ_{dc} is both in good agreement. The switch over from the frequency-independent region to frequency-dependent region is the signature of onset of conductivity relaxation.[41] The plot exhibits the typical behavior of ionic materials, i.e., the DC plateau and the frequency-dependent region.[42] The observed behavior is in general agreement with the prediction of the jump relaxation model.[43–47] According to this model, at low frequencies an ion jumps from one site to its neighboring vacant site successfully contributing to DC conductivity.

CONCLUSIONS

DC conductivity study on PUR and the Arrhenius dependence suggest a charge carrier diffusion-controlled conductivity mechanism. From the Arrhenius plots, the activation energies of the material below T_g were obtained. The activation energies increase as the oleic acid content and NCO/OH ratio increases. DC conductivities obtained for the samples were in the range of 10^{-8} to 10^{-12} Sm^{-1}. There were several conduction mechanisms occurring in the material. The analysis of DC conductivity data shows that the transport of charge carriers in the investigated system is through ionic hopping mechanism. The hyperbolic sine function was used to estimate the hopping parameters $\lambda(T)$ for PUR of this study. It is presumed that the conduction mechanism is assisted by ions for all the PURs. The ions were contributed by oleic acid due to dissociation of protons which originated from oleic acid content and highly polar urethane groups in the PURs. The frequency dependent conductivity of PUR materials has been analyzed using a Jonscher's power law expression to compare the validity of the σ_{dc}, values which have been obtained experimentally. The frequency dependent permittivity shows dielectric dispersion and the variation of dielectric constant with frequency is ascribed to the contribution of charge carriers.

References

1. Dillip, K. P., Choudhary, R. N. P., Samantaray, B. K., Karan, N. K., Katiyar, R. S., Int J Electro Chem Sci 2007, 2, 861.
2. Shin-Ichi, H., et al. J Polym Sci B Polym Phys 2005, 43, 2951.
3. Mierzwa, M.; Floudas, G., et al. Phys Rev E 2001, 64, 031703.
4. Frubing, P.; Kruger, H.; Goering, H.; Gerhard-Multhaupt, R. Polymer 2002, 43, 2787.
5. Savelyev, Y. V.; Arhranovich, E. R.; Grekov, A. P.; Privalko, E. G.; Korskanov, V. V.; Shtompel, V. I.; Privalko, V. P.; Pissis, P.; Kanapitsas, A. Polymer 1998, 39, 3425.
6. Pissis, P.; Kanapitsas, A.; Savelyev, Y. V.; Arhranovich, E. R.; Privalko, E. G.; Privalko, V. P. Polymer 1998, 39, 3431.
7. Cheng, Z. Y.; Gross, S.; Su, J.; Zhang, Q. M. J Polym Sci Phys 1999, 37, 983.
8. Korzhenko, A.; Tabellout, M.; Emery, J. R. Polymer 1999, 40, 7187.
9. Roussos, M.; Konstantopoulou, A.; Kalogeras, I. M.; Kanapitsas, A.; Pissis, P.; Savelyev, Y. V.; Vassilikou-Dova, A. E-Polym 2004, art no. 042.
10. Jahromi, S.; Litvinov, V.; Coussens, B. Macromolecules 2001, 34, 1013.
11. Oertel, G. Polyurethane Handbook, 2nd ed.; Munich: Hanser, 1994.
12. Hamid, Y.; Mohammad, R. M. Eur Polym Mater 2004, 40, 1233.
13. Ni, B.; Yang, L.; Wang, C.; Wang, L.; Finlow, D. E. J Thermal Anal Calorimetry 2010, 100, 239.
14. Güner, F. S.; Gümüsel, A.; Calica, S.; Erciyes, A. T. J Coat Technol 2002, 74, 55.
15. Manawwer Alam, S. M.; Ashraf; Ahmad, S. J Polym Res 2008, 15, 343.
16. Kong, X.; Yue, J.; Narine, S. S. Biomacromolecules 2007, 8, 3584.
17. Narine, S. S.; Yue, J.; Kong, X. J Am Oil Chem Soc 2007, 84, 173.
18. Javni, I.; Petrovic, Z. S.; Guo, A.; Fuller, R. J Appl Polym Sci 2000, 77, 1723.
19. Velayutham, T. S.; Abd Majid, W. H.; Ahmad, A. B.; Gan, Y. K.; Gan, S. N. J Appl Polym Sci 2009, 112, 3554.
20. Velayutham, T. S.; Abd Majida, W. H.; Ahmad, A. B.; Gan, Y. K.; Gan, S. N. Prog Organic Coat 2009, 66, 367.
21. Patton, T. C. Alkyd Resin Technology; Interscience Publication, New York, 1962.
22. Gowri Krishna, J.; Josyulu, O. S.; Sobhanadri, J.; Subrahmaniam, R. J Phys D Appl Phys 1982, 15, 2315.
23. Ramanarayanan, T. A.; Singhal, S. C.; Wachsman, E. D. Electrochem Soc Interf 2001, Summer, 22.

24. Mott, N. F.; Gurney, R. W. Electronic Processes in Non-Crystalline Materials; Oxford UP: London, 1948.
25. Arif, M.; Yun, M.; Gangopadhyay, S.; Ghosh, K.; Fadiga, L.; Galbrecht, F.; Scherf, U.; Guha, S. Phys Rev B 2007, 75, 195202.
26. Yoo, K. H.; Kang, K. S.; Chen, Y.; Han, K. J.; Kim, J. Nanotechnology 2008, 19, 505202.
27. Sivaraman, S.; Anantharaman, M. R. J Phys D Appl Phys 2010, 43, 055403.
28. Hill, R. M. Philos Mag 1971, 23, 59.
29. Ieda, M.; Sawa, G.; Kato, S. J Appl Phys 1971, 42, 3737.
30. Ikezaki, K.; Kanebo, T.; Sakakibara, T. Jpn J Appl Phys 1981, 20, 609.
31. Kim, D. W.; Yoshino, K. J Phys D Appl Phys 2000, 33, 464.
32. Das-Gupta, D. K.; Doughty, K.; Brockley, R. S. J Phys D Appl Phys 1980, 13, 2101.
33. Das-Gupta, D. K.; Joyner, K. J Phys D Appl Phys 1976, 9, 2041.
34. Alagiriswamy, A. A.; Narayan, K. S.; Raju, G. J Phys D Appl Phys 2002, 35, 2850.
35. Murthy, S. S. N. J Phys D Appl Phys 1988, 21, 1171.
36. Jonscher, A. K. Nature 1977, 267, 673.
37. Hamid, Y.; Mohammad, R.-N.; Mehdi, G. Polym Adv Technol 2008, 19, 1024.
38. Abd El All, S. J Phys D Appl Phys 2007, 40, 6014.
39. Fernández, M.; Landa, M.; Muñoz, M. E.; Santamaría, A. Int J Adhes Adhes 2010, 30, 609.
40. Rwei, S.-P.; Wang, L. Colloid Polym Sci 2007, 285, 1313.
41. Anantha, P. S.; Hariharan, K. Mater Sci Eng 2005, B121, 12.
42. Murugaraj, R.; Govindaraj, G.; George, D. Mater Lett 2003, 57, 1656.
43. Funke, K. Solid State Ionics 1997, 94, 27.
44. Dyre, J. C.; Schrøder, Th. B. Phys Stat Sol 2002, B230, 5.
45. Kulkarni, A. R.; Lunkenheimer, P.; Loidl, A. Solid State Ionics 1998, 112, 69.
46. Rolling, B. Solid State Ionics 1998, 105, 185.
47. Dyre, J. C. J Appl Phys 1988, 64, 2456.